European Journal of Computational Mechanics, 2014
Vol. 23, Nos. 3–4, 161–177, http://dx.doi.org/10.1080/17797179.2014.945324

Taylor & Francis
Taylor & Francis Group

Geometrically nonlinear dynamic analysis of thin shells by a four-node quadrilateral element with in-plane rotational degree of freedom

D. Boutagouga[a]* and K. Djeghaba[b]

[a]*Laboratoire des Mines, University of Tebessa, Tebessa, Algeria;* [b]*LGC, Laboratoire de génie civil, University of Annaba, Annaba, Algeria*

A simple and effective finite element incremental formulation based on the updated lagrangian corotational description for geometrically nonlinear dynamic analysis of shell structure is presented in this work. The flat shell element used is the classical four-node quadrilateral *DKQ* shell finite element, combined with the improvements of the in-plane behaviour by incorporation of the drilling rotation degree of freedom. The main goal is to have a good flat shell element of quadrilateral geometry, leading to reliable solutions in linear and geometrically nonlinear dynamic analysis. The Newmark's direct time integration method is adopted to integrate the equations of motion, while the Newton–Raphson method is used for iterating within each time step increment until equilibrium is achieved. The results obtained through a series of selected examples demonstrate the effectiveness of the used shell finite element to predict the nonlinear dynamic response of complex structures, and the robustness of this nonlinear dynamic investigation taking account of both linear and non-linear dynamic problems.

Keywords: shells; plates; nonlinear dynamic analysis; quadrilateral; drilling rotation; Newmark; finite elements

1. Introduction

Among the considerable number of shell elements that have been developed since the sixties, simple and efficient plate/shell elements are taken as prerequisite, especially for the treatment of linear and nonlinear dynamic problems. Moreover, among various flat shell elements developed in displacement formulation, the discrete Kirchhoff elements appear most attractive, where the *DKQ* flat shell element has been one of the most accuracy elements and widely used especially in static analyses. Nevertheless, quadrilaterals four-node elements are omitted in geometrically nonlinear analyses based on the updated lagrangian formulation, where the equilibrium equation is made in an updated deformed configuration. This is because the fact that the geometry resulting from the actualisation of nodal coordinates after deformation returns warped quadrilateral elements. Indeed, in general case, the four points presenting the element's nodes are not necessarily on the same plane. It is clear that due to that fact, only triangular elements could be used for the division of an arbitrary doubly curved surface into flat elements. Only few shells of simple geometry could be well presented using flat elements of quadrilateral shape with respect to the non-presence of warped elements;

*Corresponding author. Email: d.boutagouga@yahoo.fr

© 2014 Taylor & Francis

hence, in nonlinear dynamic analysis, researchers still prefer triangular elements (Argyris, Papadrakakis, & Mouroutis, 2003; Kang, Zhang, & Wang, 2009; Neto, Leal, & Yu, 2012; and Pajot & Maute, 2006). Therefore, based on the improvements that can be made by adoption of a corotational spatial local system of axes, which adapts well to the problems of quadrilateral elements, the improved *DKQ* shell element by incorporation of the drilling rotation (*d.o.f*) will be extended herein, to the development of geometrically nonlinear dynamic analysis of thin shells. Thus, the in-plane drilling rotation will be involved in a nonlinear dynamic formulation, using an updated corotational Lagrangian description.

The present investigation has been focused on the following steps:

- Formulation of a simple quadrilateral shell element with incorporation of the in-plane rotational (*d.o.f*) well known as "drilling rotation".
- Extension of this element to take into account linear and geometrically nonlinear dynamic analysis. The static extension is mainly based on the work of (Boutagouga, Gouasmia, & Djeghaba, 2010).

2. Linear shell element

The shell element studied here, is a four-node quadrilateral flat shell element. This finite element is a combination of the *DKQ* quadrilateral plate-bending element (Batoz & Ben Tahar, 1982), and Allman's-type quadrilateral plane-stress element (Ibrahimbegovic, Taylor, & Wilson, 1990). The degrees of freedom at each one of the four corner nodes are (w, θ_x, θ_y) for bending behaviour and (u, v, θ_z) for in-plane behaviour (Figure 1). In this case, the in-plane rotational degree of freedom θ_z is included in the plane-stress theory formulation as an effective degree of freedom. The considered plane-stress element is based on the Hughes's simplified variational formulation (Hughes, & Brezzi, 1989; Hughes, Brezzi, Masud, & Harari, 1989). An Allman's-type displacement field with independent interpolation of the in-plane rotation is used (Allman, 1984). The main feature of this formulation is the enhancement of the in-plane displacement field, which becomes parabolic due to the in-plane rotations effect.

As this quadrilateral shell element proves a good in-plane behaviour and, particularly, simple from the point of view of formulation, it will be extended in this work to the development of a geometrically nonlinear dynamic analysis, where a direct time integration scheme is adopted using updated corotational Lagrangian formulation.

3. Nonlinear dynamic analysis

Dynamic analysis is based on the resolution of the differential equations of motion, which can be written in the following matrix notation form:

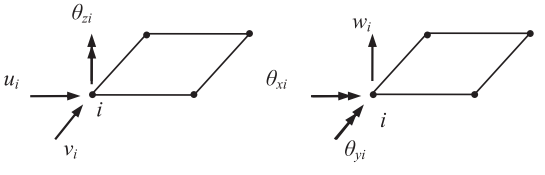

Figure 1. Four-node shell element with "Drilling Rotation".

$$M\ddot{u} + C\dot{u} + Ku = P \tag{1}$$

where the initial conditions are: $u(0) = u_0, \dot{u}(0) = \dot{u}_0$.

M, C and *K*: The overall mass, damping and stiffness matrices, respectively.

u and *P* are time-dependent vectors, where *P* represents the applied loads, and *u* represents the displacement.

In order to solve the above transitory system, direct time integration methods are widely used. This involves the attempt to satisfy dynamic equilibrium at discrete points in time, where the problem is solved step-by-step using numerical integration algorithm. A wide variety of numerical methods have been proposed where they differ by the manner used to express the relationship between displacement, velocity and acceleration (Bert, & Stricklin, 1988; Dokainish, & Subbaraj, 1989; Subbaraj, & Dokainish, 1989). However, all methods can fundamentally be classified as either explicit or implicit integration methods. Generally, implicit algorithms are most effective for structural dynamic problems (low-frequency modes), while explicit algorithms are very efficient for wave propagation problems (high-frequency modes).

In this investigation, we used the single step implicit Newmark's method. In this subject, the equation (1) is considered at time $(t+\Delta t)$ as:

$$M\ddot{u}_{t+\Delta t} + C\dot{u}_{t+\Delta t} + Ku_{t+\Delta t} = F_{t+\Delta t} \tag{2}$$

where $u_{t+\Delta t}$ $\dot{u}_{t+\Delta t}$ and $\ddot{u}_{t+\Delta t}$ are, respectively, the $u(t+\Delta t), \dot{u}(t+\Delta t), \ddot{u}(t+\Delta t)$ approximations at time $(t+\Delta t)$. The method is implicit, which means that the solution at time (t) is required to satisfy the differential equation of equilibrium at time $(t+\Delta t)$. The method requires the solution of a set of simultaneous equations at each time step. To begin the iterative process, we must first calculate $\ddot{u}_0$, where:

$$M\ddot{u} = F_0 - C\dot{u}_0 - Ku_0 \tag{3}$$

The Newmark's process equations are written in the following form:

$$\begin{cases} \dot{u}_{t+\Delta t} = b_1(u_{t+\Delta_t} - u_t) + b_2\dot{u}_t + b_3\ddot{u}_t \\ \dot{u}_{t+\Delta t} = b_4(u_{t+\Delta_t} - u_t) + b_5\dot{u}_t + b_6\ddot{u}_t \end{cases} \tag{4}$$

Substituting Equation (4) into Equation (2) allows dynamic equilibrium at time $(t+\Delta t)$ to be written in terms of the unknown node displacements as:

$$(b_1M + b_4C + K) = F_{t+\Delta t} + M(b_1u_t - b_2\dot{u}_t - b_3\dot{u}_t) + C(b_4u_t - b_5\dot{u}_t - b_6\dot{u}_t) \tag{5}$$

where the constants b_1:–b_6 are defined as: $b_1 = \frac{1}{\beta\Delta t^2}$; $b_2 = \frac{-1}{\beta\Delta t}$; $b_3 = 1 - \frac{1}{2\beta}$; $b_4 = \gamma\Delta t\ b_1$; $b_5 = 1 + \gamma\Delta t$; and $b_6 = \Delta t(1 + \gamma b_3 - \gamma)$.

With β and γ as parameters that control the stability and accuracy of the algorithm. $\gamma = 1/2$ and $\beta = 1/4$.

The matrix $k\sim = k + b_1M + b_4C$ is considered as the effective stiffness matrix. It is formed and triangularised only once for linear analysis. In the other side, the effective load vector is:

$$\bar{F}_{t+\Delta t} = F_{t+\Delta t} + M(b_1u_t - b_2\dot{u}_t - b_3\ddot{u}_t) + C(b_4u_t - b_5\dot{u}_t - b_6\ddot{u}_t) \tag{6}$$

Extension of Newmark's method to nonlinear dynamic analysis requires that iterations must be performed at each time step (Δt) to obtain the nonlinear response satisfying the equilibrium equations. Incremental tangent stiffness matrix is used; it must be formed and triangularised at each iteration.

In order to extend the linear dynamic scheme to take account for geometrically nonlinear behaviour, equilibrium equation of motion must be taken as:

$$M\ddot{u}_{t+\Delta t} + C\dot{u}_{t+\Delta t} + N(u)_{t+\Delta t} = R_{t+\Delta t} \tag{7}$$

where $R_{t+\Delta t}$is the nodal residual forces vector at time $(t+\Delta t)$.

$N(u)_{t+\Delta t}$ is the equivalent internal forces vector at time $(t+\Delta t)$, it is written as:

$$N(u)_{t+\Delta t} = \int_v [B_{t+\Delta t}]^T \{\sigma(\epsilon)_{t+\Delta t}\} dv \tag{8}$$

Equation (7) can be solved using the same step-by-step integration method used for linear dynamic analysis. At which, the Newton–Raphson algorithm is employed for iterating within each time step increment until equilibrium is achieved.

3.1. *Tangent stiffness matrix*

When updated corotational formulation is considered, the configuration $C_{t+\Delta t}$ to be calculated is obtained starting from the configuration C_t considered as known. In general, we can define four positions that a solid can occupy during its movement (Figure 2).

where γ^{o} is the initial undeformed configuration;

γ^{n-1}: the actual deformed configuration;

γ^{n}: configuration to be calculated; and

$\gamma \sim^{n-1}$: configuration very close to γ^{n-1} obtained after a rigid body movement of γ^{o}.

In incremental way, Green's strain tensor that represents a shell element is written as:

$$\Delta e_{ij} = \frac{1}{2}\left(\frac{\partial \Delta u_i}{\partial x_j} + \frac{\partial \Delta u_j}{\partial x_i}\right) - z\frac{\partial^2 \Delta w}{\partial x_i \partial x_j} + \frac{1}{2}\left(\frac{\partial \Delta w}{\partial x_i}\frac{\partial \Delta w}{\partial x_j}\right) \tag{9}$$

The equilibrium equation is obtained by the application of the virtual work principle in incremental form between the configurations $\gamma \sim^{n-1}$ and γ^{n}:

$$\int_{\bar{v}} (T_{ij}\delta(\Delta\epsilon^*_{ij}) + D_{ijkl}\Delta\epsilon_{ij}\delta(\Delta\epsilon_{ij}))d\bar{V} = W_{\text{ext}} - \int_{\bar{v}} T_{ij}\delta(\Delta\epsilon_{ij})d\bar{V} \tag{10}$$

where $\Delta\epsilon_{ij}; \Delta\epsilon^*_{ij}$ are the linear and nonlinear parts of the incremental Green's strain tensor;

T_{ij} is the Cauchy stress; and: D_{ijkl} is the linear elasticity Matrix.

Using the same shape functions defined for the finite shell element in linear analysis, the tangent stiffness matrix $[K_T]$ is written as:

$$\int_{\bar{v}} (T_{ij}\delta(\Delta\epsilon^*_{ij}) + D_{ijkl}\Delta\epsilon_{ij}\delta(\Delta\epsilon_{ij}))d\bar{V} = \{\delta(\Delta q)\}^T[K_T]\{\Delta q\} \tag{11}$$

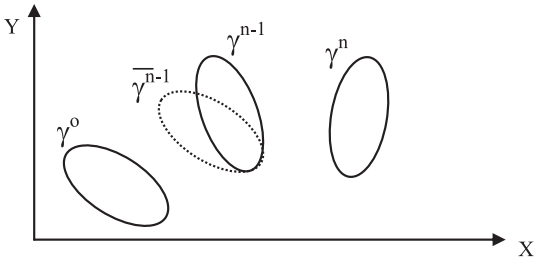

Figure 2. Configurations of a moving solid.

$$\text{where : } [K_T] = [K_0] + [K_\sigma] \tag{12}$$

$[K_0]$: the small displacement matrix
$[K_\sigma]$: the initial stress matrix
The internal forces $\{F_{int}\}$ are such as:

$$\int_{\bar{v}} T_{ij}\delta(\Delta\varepsilon_{ij})d\bar{V} = \{\delta(\Delta q)\}^T\{F_{\text{int}}\} \tag{13}$$

Residual force and internal force vectors are expressed in the updated configuration at time (t) as:

$$\begin{cases} {}^t_tR = {}^t_tP - \int_v {}^tT_{ij} \cdot {}^tB_{ij} \cdot dv \\ {}^t_tF_{\text{int}} = \int_v {}^tT_{ij} \cdot {}^tB_{ij} \cdot dv \end{cases} \tag{14}$$

Strain tensor is calculated in relation to the reference plane related to the corotational reference system, which is continuously updated.

3.2. *Initial stress matrix*

Initial stress matrix is calculated using stress field resulting from the previous configuration and quadratic terms of the nonlinear Green-Lagrange strain as:

$$[K_\sigma] = \int_A [g]^T[C][g]d\ {}^tA \tag{15}$$

where $[C]$is the in-plane (membrane) stress tensor

$$[C] = \begin{bmatrix} N_{xx} & N_{xy} \\ N_{yx} & N_{yy} \end{bmatrix} \tag{16}$$

Quadratic terms of the nonlinear Green-Lagrange strain are written as:

$$\{\varepsilon^{nl}\} = \frac{1}{2}\{q\}[g]^T[g]\{q\} \tag{17}$$

$[g]$: represents the slope matrix; it is expressed as a function of bending derivatives:

$$[g]\{\Delta q\} = \begin{bmatrix} \frac{\partial w}{\partial x} \\ \frac{\partial w}{\partial y} \end{bmatrix} \tag{18}$$

$$[g] = \begin{bmatrix} \frac{\partial N}{\partial x} \\ \frac{\partial N}{\partial y} \end{bmatrix} \tag{19}$$

where N represents shape functions.

It is well known that *DKQ* element has no explicit expression for bending displacement (w). Therefore, bi-cubic polynomial interpolation is necessary and sufficient. The adopted polynomial and the resulting shape functions are presented in Appendix A.

3.3. *Nonlinear recurrence scheme*

The various steps to be taken into account for the nonlinear dynamic incremental approach using the corotational updated Lagrangian description are:

***1**-Initial Calculations*

- Select time step Δt and calculate b_i constants
- Form the matrices K, M and C
- Initialise $u(0) = u_0, \dot{u}(0) = v_0$ and solve for initial acceleration: $M\ddot{u}_0 = F_0 - C\dot{u}_0 - Ku_0$

***2**-For Each Time Step*

- calculate tangent stiffness matrix $K_t = \int_{\bar{v}} B_t^T D B_t dv$
- form and triangularise the effective stiffness matrix $\bar{K} = K + b_1 M + b_4 C$
- form the effective load vector $\bar{F}_{t+\Delta t}$

***3**-For Each Iteration*

- solve for displacements at $(t + \Delta t)$: $\bar{K}\Delta u_{t+\Delta t} = R_{t+\Delta t}$
  - before evaluation of the tangential stiffness and internal forces, we update the new system axis on the preceding position of the element nodes
  - the internal strains and stresses are calculated in the new reference system of the precedent step
  - the new solution is obtained after linearisation of the problem by calculating the internal strains and stresses in the new reference system of the precedent step
  - the solution is used to proceed to the next step.
- check for convergence of the iteration process (if *OK* continue, else go to **3**)
- Calculate velocities and accelerations at $(t + \Delta t)$
- $\begin{cases} \ddot{u}_{t+\Delta t} = b_1(u_{t+\Delta} - u_t) + b_2\dot{u}_t + b_3\ddot{u}_t \\ \dot{u}_{t+\Delta t} = b_4(u_{t+\Delta} - u_t) + b_5\dot{u}_t + b_6\ddot{u}_t \end{cases}$
- $t = t + \Delta t$
- go to ***2***

4. Corotational formulation

The corotational description is used in order to decompose the motion of an element into small (deformational) displacement and (strain free) rigid body motion parts. After extracting rigid body displacements and rotations, the small displacement part is dealt using the linear stiffness. In this case, the finite element developed for linear analysis in small displacements can be applied to nonlinear dynamic analysis with large displacements and rotations.

In order to captivate rigid body motion, a corotational reference system is used, its axes make rotations and translations with the element movement. The deformation is always measured on the level of the element's local system since large translations and large rotations are absorbed by the corotational system of axes, which continuously rotates and translates with the element movement.

Small deformational displacements d are defined by extracting the rigid body motion from the global displacements d_g. So, small displacements are expressed as function of global and rigid body displacements as:

$$d = d_g - d_R$$

In purpose to well handle the problems related to the probably nonplanarity of the deformed quadrilateral's nodes, we attached the middle surface of quadrilateral shell element to a local reference system ***oxyz***, as illustrated in Figure 3, in which the ***x***-axis contains both points ***a*** and ***b*** located at halfway of lines (1–4, 2–3) and the ***y***-axis is perpendicular to the ***x***-axis; the two axes cross at point **o** located at halfway of the line (***a***–***b***).

The out of plane rigid body displacements and rotations are handled as presented in (Boutagouga et al., 2010).

All coordinates and displacements are measured in the initial local (*XY)* plane of the considered finite element.

We denote by ${}^0X_O, {}^0Y_O$ the coordinates of the central point "**o**" at the initial configuration at time ($t = 0$). They are defined as:

$$ {}^0X_O = \frac{\sum_{i=1}^{4} {}^0X_i}{4}, \; {}^0X_O = \frac{\sum_{i=1}^{4} {}^0Y_i}{4} \tag{20} $$

After having displacement, the coordinates of the central point "**o**" at time (t) are denoted as ${}^tX_O, Y_O$, respectively:

$$ {}^tX_O = {}^0X_O + \frac{\sum_{i=1}^{4} U_i}{4}, \; {}^tY_O = {}^0Y_O + \frac{\sum_{i=1}^{4} V_i}{4} \tag{21} $$

In-plane rigid body displacements are calculated via two steps. First, we calculate U_O, V_O, which are the rigid translations of the central point "**o**" (Figure 4). They are defined as:

$$ U_O = \frac{\sum_{i=1}^{4} U_i}{4}, V_O = \frac{\sum_{i=1}^{4} V_i}{4} \tag{22} $$

In the second step, we calculate additional displacements U_i^*, V_i^* introduced by the rigid rotation $\varnothing_o$ of the "***x***" axis (Figure 5), they are calculated as:

$$ \begin{cases} U_i^* = {}^tX_i - {}^0X_i \\ V_i^* = {}^tY_i - {}^0Y_i \end{cases} \tag{23} $$

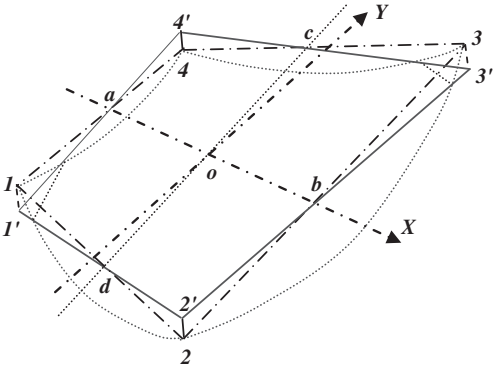

Figure 3. Chosen reference position.

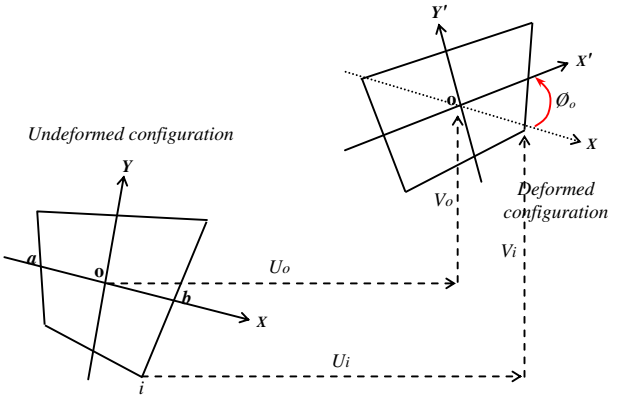

Figure 4. In-plane rigid body translations of the element's centre.

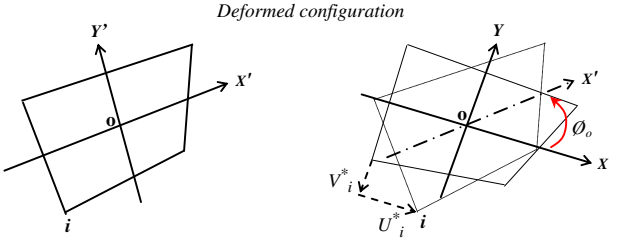

Figure 5. In-plane rigid body rotation of the "x" axis.

Finally, rigid translations vector is defined by:

$$\begin{Bmatrix} U_i^R \\ V_i^R \end{Bmatrix} = \begin{Bmatrix} U_O + U_i^* \\ V_O + V_i^* \end{Bmatrix} \tag{24}$$

For the evaluation of in-plane rigid body rotations related to the drilling rotations (*d.o.f*), we should note that we could not use the average rigid rotation $\varnothing o$ of the whole element, because each node has a different rigid rotation.

The drilling degree of freedom may be physically interpreted as the rotation of the vertex bisecting the angle between adjacent edges. Hence, the in-plane rigid body rotations are interpreted as the rigid body rotations of the vertexes bisecting the angles between adjacent edges.

Assuming that the element's sides remain rectilinear, let us calculate φ_i^R as illustrated by Figure 6, where the rigid in plane rotation of node (i) is written as:

$$\varnothing_i^R = \left(\varphi_{ij}^R + \varphi_{ki}^R\right)/2 \quad i = 1,2,3,4;\ j = 2,3,4,1;\ k = 4,1,2,3. \tag{25}$$

φ_{ij}^R is the rigid rotation of an edge (*ij),* which is calculated from the global coordinates of nodes *(i)* and *(j)* as*:*

$$\varphi_{ij}^R = \operatorname{atan}\frac{{}^tY_j - {}^tY_i}{{}^tX_j - {}^tX_i} - \operatorname{atan}\frac{{}^0Y_j - {}^0Y_i}{{}^0X_j - {}^0X_i} \tag{26}$$

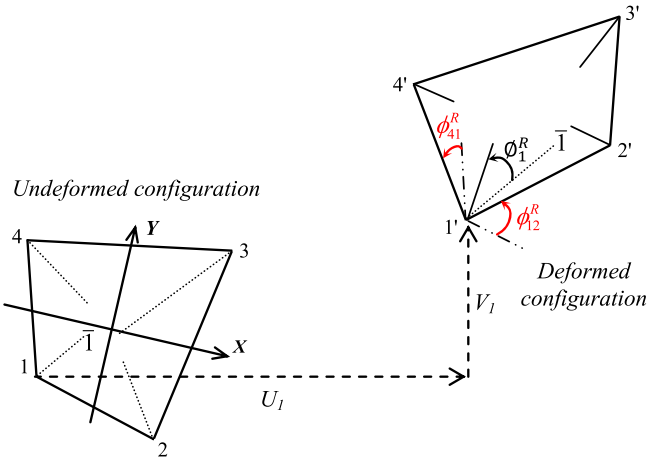

Figure 6. In-plane rigid body rotations.

with ${}^tX_i = {}^0X_i + U_i$, and ${}^tY_O = {}^0Y_O + V_i$.

After having local deformational displacements, they are used in order to compute the internal force vector and tangent stiffness matrix K_T.

5. Numerical results

In this section, some dynamic analysis of several plate and shell structures have been carried out to demonstrate the efficiency of the proposed approach in linear and geometrically nonlinear dynamic analysis.

In the frame of this research work, the data processing developments enabled us to have a finite elements programme written in Fortran language for PC devoted to the geometrically nonlinear dynamic analysis of plate/shell structures. Using this programme, the analyses may be carried out using one of the two following finite elements:

"*Quad*": quadrilateral flat shell finite element with fictitious stiffness (*DKQ* + Quadrilateral membrane element + fictitious stiffness).

"*Qdrill*": quadrilateral flat shell finite element with drilling rotation (*DKQ* + Quadrilateral membrane element incorporing the in-plane rotational degrees of freedom).

In all presented examples, the material behaviour is taken to be isotropic and linearly elastic. The damping ratio is taken to be null.

Numerical comparisons are drawn between the developed element and the existing solutions available in literature. These comparisons demonstrate the validity and reliability of the proposed approach.

5.1. *Simply supported rectangular plate under concentrated step load*

The first example considers the linear and geometrically nonlinear dynamic analysis of a rectangular plate of $l = 1524$ mm long and $w = 1016$ mm wide, with simply supported edges (Figure 7). The plate is subject to the time-dependent concentrated load shown in Figure 8, which is applied at the centre of the plate, with $\boldsymbol{P_0} = 44.54\,N$ and $t_0 = 0.006$ s.

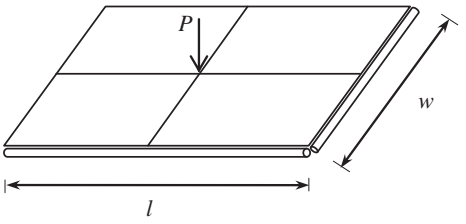

Figure 7. Geometry of the simply supported plate.

Because of the double symmetry of geometry, loading and boundary conditions, only one-quarter of the plate is required to perform the example.

The thickness is taken as $h = 25.4$ mm, Young's modulus of elasticity of the material is $E = 2.0955 \times 10^8$ N/m^2, the specific weight is $\rho = 3210.05$ kg/m^3 and the Poisson's ratio is $\upsilon = 0.25$.

For direct integration of this example, the time step size was taken $\Delta t = 0.004$ s.

The computed displacement time history of the central point, using the two elements with 8×8 mesh, is shown in Figure 9. The first observation we made is that the "*Quad*" and "*Qdrill*" elements give exactly the same results in linear dynamic analyses, and very close results in geometrically nonlinear analyses. Also, it is observed that "*Quad*" element and "*Qdrill*" element give a very good accurate results accordingly to the results of (Meek, & Wang, 1998) in both, linear and geometrically nonlinear dynamic analysis.

In this example, the nonlinear dynamic process using "*Quad*" and "*Qdrill*" elements necessitate two iterations at each time step to perform the test, which mean that there is no highly nonlinear behaviour, but it has been clearly observed from Figure 9 that the nonlinear effect is predominant.

5.2. *Simply supported square plate under uniform step pressure*

The second example considers the square plate shown in Figure 10 that is subjected to a suddenly applied uniform pressure shown in Figure 11.

The plate dimensions are: $a = 254$ mm, $h = 12.7$ mm, It is simply supported at the four edges, and it has the following material properties: modulus of elasticity $E = 68950$ MPa, Poisson's ratio $\upsilon = 0.3$ and mass density $\rho = 2765.8$ kg/m^3.

Using double symmetry, only 4×4 shell elements are used to model one-quarter of the plate.

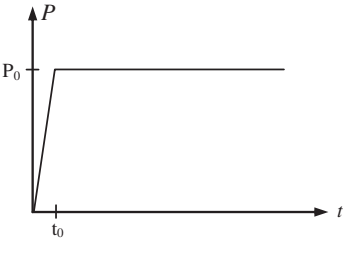

Figure 8. Concentrated step load.

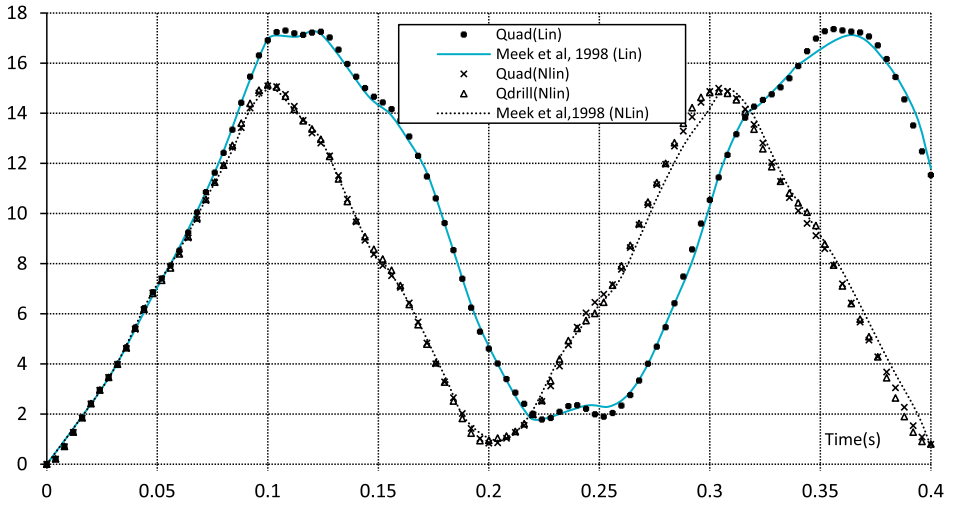

Figure 9. Central point deflection time history of the rectangular plate.

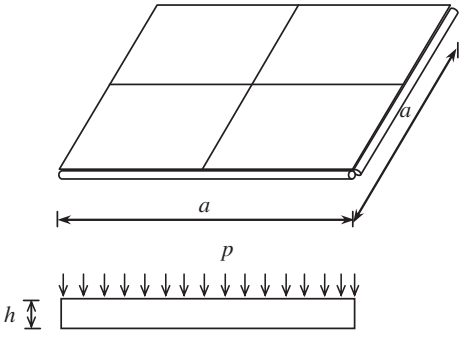

Figure 10. Geometry and loading of the square plate.

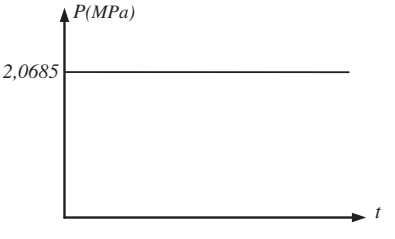

Figure 11. Suddenly applied uniform pressure.

The linear and nonlinear vertical displacement time histories of the central point of this plate are represented in Figure 12. In order to check our results, we referred to the solution of Ali and Al-Noury (1986) where they solved the problem by finite difference method. We noticed that a close agreement has been found with the results of Ali and Al-Noury (1986).

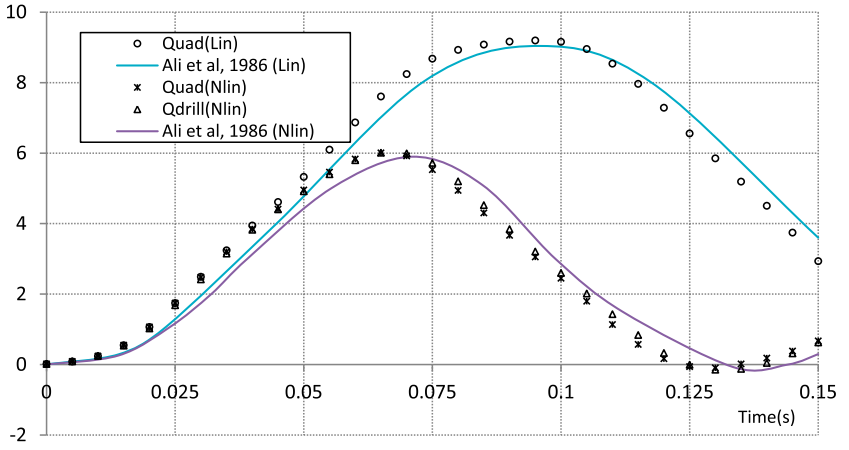

Figure 12. Central point deflection time history of the square plate.

The total number of iterations that requires *"Qdrill"* element to plot the curve presented at Figure 12 is 73 iterations, while the *"Quad"* elements requires 77 iterations. For both elements, most time steps need three iterations in exception of some time-steps that need four iterations in the case when we used *"Quad"* element.

In this example, which is a plate structure, where bending is dominating, "*Quad*" element needed some extra iterations to achieve equilibrium immediately when the structure exhibits moderate nonlinearity. Contrary, "*Qdrill*" element was more effective even when the in-plane behaviour is dominated by bending behaviour.

5.3. Thin cylindrical shell under uniformly distributed half sin wave loading

A thin cylindrical shell structure having the geometry shown in Figure 13 is studied in this example. Central point vertical displacement is drawn when the shell is subjected to a uniformly distributed half sinusoidal wave loading with a peak intensity of 4309.2 N/m^2 shown in Figure 14.

The two straight edges of the shell are free while the curved edges are supported on rigid diaphragms against the in-plane degrees of freedom (u, w, θ_y). The shell geometrical, mechanical and physical characteristics are taken as follows:

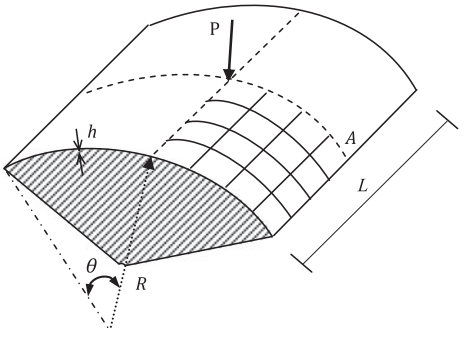

Figure 13. Geometry of the cylindrical shell.

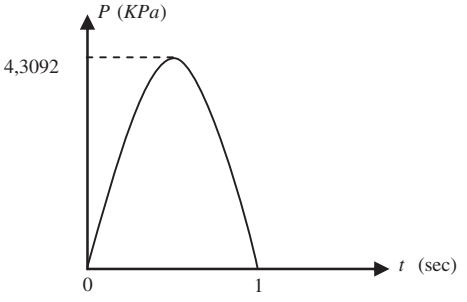

Figure 14. Half-sinusoidal loading.

Radius of curvature $R = 15240$ mm, longitudinal length $L = 15240$ mm, thickness $h = 76.2$ mm, opening angle $\theta = 20^{o}$, poisson's ratio $\nu = 0.3$, modulus of elasticity $E = 20685$ MPa and weight density $\rho = 1.795$ kPa.

In this example, a complete study has been done. The predominance of nonlinearity has been shown over linear response. The vertical deflection time history curves of the midpoint of the free edge (point A) are shown in Figures 15 and 16. They show that there is good agreement between the present solutions using 4x4 shell elements by both shell elements and Clough and Wilson (1971) results.

First, we should note that there is a remarkably softness in the "*Qdrill*" element results in comparison with the other elements results in both linear and nonlinear dynamic analysis. That can be explained by the fact that "*Qdrill*" element gives ameliorated in-plane behaviour. That amelioration occurs as a softening in the structure when it has some parts under bending applied in the plane of the shell elements, which is not the case when we use classical shell elements.

Secondly, all time steps need three iterations to achieve equilibrium with both elements, because the structure in this case is stiffened by the diaphragm and the behaviour is not highly nonlinear by consequence.

5.4. Hinged cylindrical panel under a concentrated load

A thin cylindrical shell of radius of curvature R, longitudinal length L, thickness h and opening angle θ is shown in Figure 17. Its curved edges are free while its straight

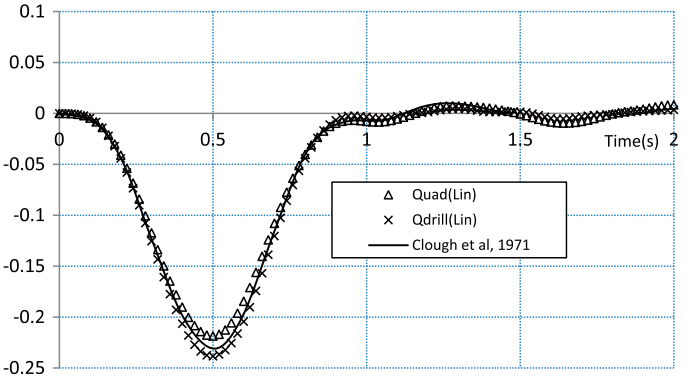

Figure 15. Deflection time history of point A (linear analysis).

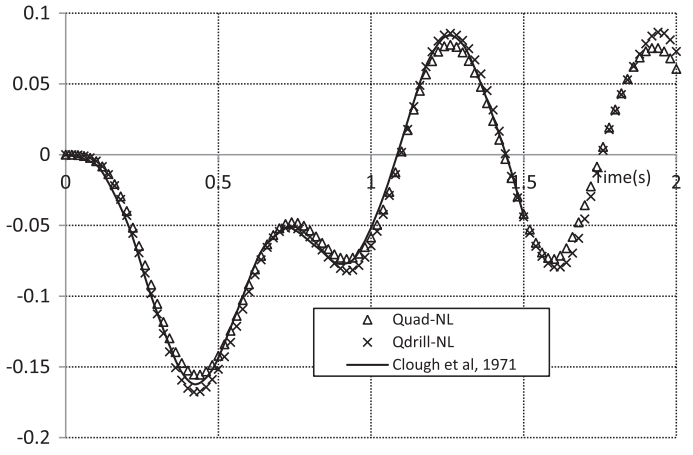

Figure 16. Deflection time history of point A (nonlinear analysis).

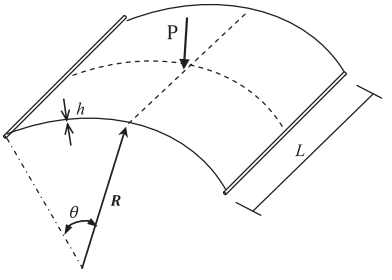

Figure 17. Geometry of the cylindrical panel.

edges are hinged. This shell structure is subjected to a concentrated load applied at the centre. Using double symmetry of the shell structure, only one quarter of the shell is modellised using 8×8 quadrilateral elements. The geometrical and mechanical characteristics are as follows:

$R = 2540$ mm; $L = 2540$ mm; $\theta = 0{,}1$ rad; $h = 6.35$ mm; $v = 0{,}30$; $E = 0.310275$ kN/mm^2; and $\rho = 3210.05$ kg/m^3.

The applied concentrated load is shown in Figure 8, with $\boldsymbol{P_0} = 400\ N$ and $t_0 = 0.01$ s. For direct integration, the time step size is $\Delta t = 0.001$ s.

The obtained deflection time history curves using "*Qdrill*" and "*Quad*" elements given in Figure 18 show that an excellent agreement with Meek and Wang (1998) solution is obtained using 8×8 quadrilateral meshing elements.

The most important factor in this study is the number of iterations required by each one of the two shell elements presented herein to perform the example. To make a comparison, the results are tabulated in Table 1.

It is easy to see that the solution obtained using "*Qdrill*" element was very faster than the solution obtained using "*Quad*" element. In this example, it is 1.2 times faster.

Also, "*Qdrill*" shell element ensures more numerical stability compared with "*Quad*" element. As we could see, "*Quad*" element needed 12 iterations within time step when highly nonlinear behaviour is exhibited, which mean that this element suffers

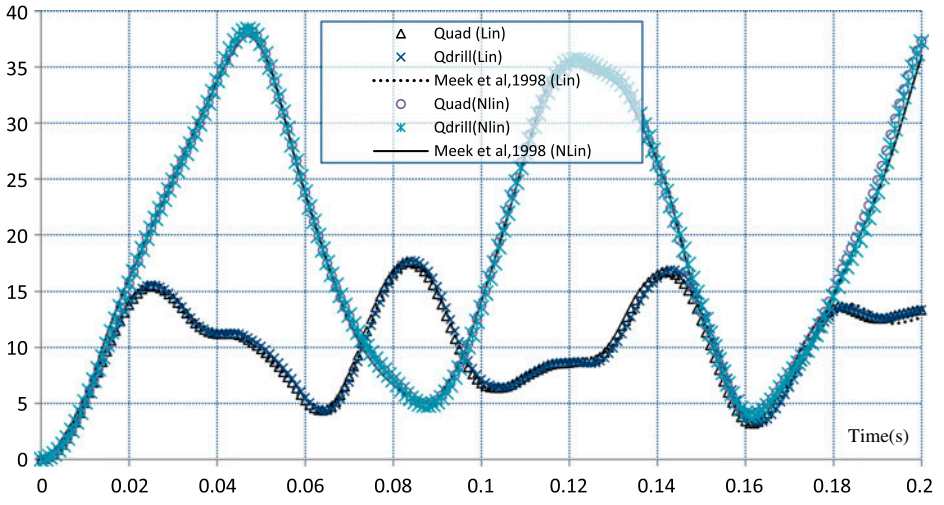

Figure 18. Central point deflection time history of the cylindrical panel.

Table 1. Iterations number cost for "*Quad*" and "*Qdrill*" elements.

Shell element	*"Quad"*	*"Qdrill"*
(Time step × Iterations number) sequence	6 × 2	6×2
	14×3	13 × 3
	8 × 2	8 × 2
	55 × 3	14 × 3
	3 × 4	3 × 2
	8 × 3	19 × 3
	3 × 2	21 × 2
	26 × 3	4 × 3
	1 × 4	12 × 2
	1 × 6	25 × 3
	1 × 12	1 × 2
	1 × 7	13 × 3
	1 × 5	5 × 2
	31 × 3	9 × 3
	3 × 4	10 × 2
	7 × 5	10 × 3
	2 × 4	12 × 2
	28 × 3	15 × 3
	1 × 4	
Total	625	522

for numerical instability, especially in regions of large nonlinearity. This could lead to divergence from the exact solution. Consequently, larger time step could be used safely using "*Qdrill*" element.

These results illustrate that "*Qdrill*" shell element is a powerful and reliable shell element that could be used for geometrically nonlinear dynamic analysis by direct time integration, especially when the structure response involves highly nonlinear behaviour.

6. Conclusion

The efficiency of the *DKQ* shell element with drilling rotation for static nonlinear analyses using an updated corotational formulation has been shown previously in (Boutagouga et al., 2010). In this paper, the effectiveness of this element in linear and geometrically nonlinear dynamic analyses using an updated corotational formulation of plate/shell structures has been presented. Several examples are solved with various types of loading. The results show a great numerical stability and less numerical cost in critical situations when the structure response involves highly nonlinear behaviour. It could be concluded from the obtained results that this element is very reliable and much efficient for geometrically nonlinear dynamic analysis of plate and shell structures. This element seems to be the better choice of the membrane part to use for flat shell finite elements. The interpolation of the in-plane rotational (*d.o.f*) has a major advantage on the flat shell element's response stability and reliability. Such a flat shell element could be a good candidate for general shell structural analysis in engineering practice.

References

Ali, S. A., & Al-Noury, S. I. (1986). Nonlinear dynamic response of rectangular plates. *Computers and Structures, 22*, 433–437.

Allman, D. J. (1984). A compatible triangular element including vertex rotations for plane elasticity analysis. *Computers and Structures, 19*, 1–8.

Argyris, J., Papadrakakis, M., & Mouroutis, Z. S. (2003). Nonlinear dynamic analysis of shells with the triangular element TRIC. *Computer Methods in Applied Mechanics and Engineering, 192*, 3005–3038.

Batoz, J. L., & Ben Tahar, M. (1982). Evaluation of new Quadrilateral thin plate bending element. *International Journal for Numerical Methods in Engineering, 18*, 1655–1677.

Bert, C. W., & Stricklin, J. D. (1988). Comparative evaluation of six different numerical integration methods for non-linear dynamic systems. *Journal of Sound and Vibration, 127*, 221–229.

Boutagouga, D., Gouasmia, A., & Djeghaba, K. (2010). Geometrically nonlinear analysis of thin shell by a quadrilateral finite element with in-plane rotational degrees of freedom. *European Journal of Computational Mechanics, 19*, 707–724.

Clough, R. W., & Wilson, E. L. (1971). Dynamic finite element analysis of arbitrary thin shells. *Computers and Structures, 1*, 33–56.

Dokainish, M. A., & Subbaraj, K. (1989). A survey of direct time-integration methods in computational structural dynamics-I. Explicit methods. *Computers and Structures, 32*, 1371–1386.

Hughes, T. J. R., & Brezzi, F. (1989). On drilling degrees of freedom. *Computer Methods in Applied Mechanics and Engineering, 72*, 105–121.

Hughes, T. J. R., Brezzi, F., Masud, A., & Harari, I. (1989). *Finite elements with drilling degrees of freedom: theory and numerical evaluations*. Fifth International Symposium on Numerical Methods in Engineering..Ashurst, UK, 3–17.

Ibrahimbegovic, A., Taylor, R. L., & Wilson, E. L. (1990). A robust quadrilateral membrane finite element with drilling degrees of freedom. *International Journal for Numerical Methods in Engineering, 30*, 445–457.

Kang, L., Zhang, Q., & Wang, Z. (2009). Linear and geometrically nonlinear analysis of novel flat shell element with rotational degrees of freedom. *Finite Elements in Analysis and Design, 45*, 386–392.

Meek, J. L., & Wang, Y. (1998). Nonlinear static and dynamic analysis of shell structures with finite rotation. *Computer Methods in Applied Mechanics and Engineering, 162*, 301–315.

Neto, M. A., Leal, R. P., & Yu, W. (2012). A triangular finite element with drilling degrees of freedom for static and dynamic analysis of smart laminated structures. Computers and Structures, 108–109, 61–74.

Pajot, J. M., & Maute, K. (2006). Analytical sensitivity analysis of geometrically nonlinear structures based on the co-rotational finite element method. *Finite Elements in Analysis and Design, 42*, 900–913.

Subbaraj, K., & Dokainish, M. A. (1989). A survey of direct tome-integration methods in computational structural dynamics- II. Implicit methods. *Computers and Structures, 32*, 1387–1401.

Appendix A.

In order to construct the bending function, we used the following polynomial expressed in the natural reference system

$$w(\xi,\eta) = 1\xi\eta\xi^2\eta^2\xi\eta\xi^3\eta^3\xi^2\eta\xi\eta^2\xi^3\eta\xi\eta^3$$

We get the following shape functions that are used to construct the slope matrix [g]:

$$N_{w1}(\xi,\eta) = \frac{1}{8}(2 - 3\xi - 3\eta + 4\xi\eta + \xi^3 + \eta^3 - \xi^3\eta - \xi\eta^3)$$

$$N_{w2}(\xi,\eta) = \frac{1}{8}(2 + 3\xi - 3\eta - 4\xi\eta - \xi^3 + \eta^3 + \xi^3\eta + \xi\eta^3)$$

$$N_{w3}(\xi,\eta) = \frac{1}{8}(2 + 3\xi + 3\eta + 4\xi\eta - \xi^3 - \eta^3 - \xi^3\eta - \xi\eta^3)$$

$$N_{w4}(\xi,\eta) = \frac{1}{8}(2 - 3\xi + 3\eta - 4\xi\eta + \xi^3 - \eta^3 + \xi^3\eta + \xi\eta^3)$$

$$N_{\theta 11}(\xi,\eta) = -\frac{1}{8}(\xi - 1)^2(\xi + 1)(\eta - 1)$$

$$N_{\theta 12}(\xi,\eta) = -\frac{1}{8}(\xi - 1)(\xi + 1)^2(\eta - 1)$$

$$N_{\theta 13}(\xi,\eta) = \frac{1}{8}(\xi - 1)(\xi + 1)^2(\eta + 1)$$

$$N_{\theta 14}(\xi,\eta) = -\frac{1}{8}(\xi - 1)^2(\xi + 1)(\eta + 1)$$

$$N_{\theta 21}(\xi,\eta) = -\frac{1}{8}(\xi - 1)(\eta - 1)^2(\eta + 1)$$

$$N_{\theta 22}(\xi,\eta) = \frac{1}{8}(\xi + 1)(\eta - 1)^2(\eta + 1)$$

$$N_{\theta 23}(\xi,\eta) = \frac{1}{8}(\xi + 1)(\eta - 1)(\eta + 1)^2$$

$$N_{\theta 24}(\xi,\eta) = -\frac{1}{8}(\xi - 1)(\eta - 1)(\eta + 1)^2$$